Changes in illumination color induce powerful illusory rotations

Pont, Sylvia; Doerschner, Katja

DOI
10.1364/JOSAA.545157

Publication date
2025

Document Version
Final published version

Published in
Journal of the Optical Society of America A: Optics and Image Science, and Vision

B124 Vol. 42, No. 5 / May 2025 / Journal of the Optical Society of America A Research Article

Journal of the Optical Society of America A
OPTICS, IMAGE SCIENCE, AND VISION

Changes in illumination color induce powerful illusory rotations

Sylvia Pont[1,†,*] and Katja Doerschner[2,†]

[1]Delft University of Technology, Industrial Design Engineering, Perceptual Intelligence Lab, Landbergstraat 15, 2628CE Delft, The Netherlands
[2]Justus-Liebig-Universität Giessen, Allgemeine Psychologie & Visuelle Neurowissenschaft, Otto-Behaghel-Str.10F, 35394 Giessen, Germany
[†]These authors contributed equally to this work.
*s.c.pont@tudelft.nl

Received 1 November 2024; revised 18 December 2024; accepted 19 December 2024; posted 20 December 2024; published 29 January 2025

We present a novel, to the best of our knowledge, interactive mechanism for inducing illusory rotations. Printed versions of Kitaoka's rotating snakes illusion change effective color contrast depending on LED illumination color. This drives changes in the illusory rotations. In a psychophysical experiment, participants indicated by button press whether they perceived a given pattern to rotate as the color of illumination changed and in which direction this rotation occurred. Results could be predicted by an effective luminance contrast model, and we found high agreement between observers. This constitutes a novel manner of showing perceptual mechanisms, allowing for new applications and adding perceptual dynamics to static imagery.

https://doi.org/10.1364/JOSAA.545157

1. INTRODUCTION

This paper presents a novel interactive mechanism for inducing illusory rotations. We found this effect by serendipity. To our big surprise, experimenting with a color-varying LED source, we found that printed illusory motion illusions in the lab started to rotate to and fro. The induced rotations are powerful, can be clockwise and anti-clockwise in a single original colored rotation illusion, and can be very well predicted. This allows for a wide range of applications, adding perceptual dynamics to static imagery.

Repeated asymmetric patterns [1], such as the rotating snakes illusion [2], induce illusory rotation. When this combination is repeated, a strong illusion can be observed in this direction. They are enhanced by moving the eyes across the pattern [3] and by color and overall contrast [4–6]. The main causes were analyzed and were found to be due to the differences in the neural processing of low- and high-contrast regions that are interpreted as velocity signals [3,4,6]. The perceived direction is usually from high to low contrast regions and is determined by the change in the neural responses over time. Others have shown that a simple motion energy model extended by nonlinearity can account for the perceived direction of illusory rotation [7]. However, this model could predict the direction but not the magnitude of the rotation effect. If the pattern repeats the order black, dark gray, white, light gray, and back to black, a strong illusion can be observed in this direction [1]. Using the cancellation method [8], we found that the velocity required to establish perceptual stationarity was greater for a stimulus composed of patterns with a blue–yellow combination than with a stimulus composed of a red–green and a grayscale variation when the luminance of corresponding elements within the patterns was equated (though chromatic saturation contrast was not controlled in their equipment). The rotating snakes illusion is greater in the periphery, is dependent on eye movements, and disappears when viewed through a pinhole aperture [9].

Another type of rotation illusion and motion illusion are dependent on dynamic contrast changes [10–14], e.g., the reverse phi effect. The "reversed phi" phenomenon was discovered by Anstis [13]. If stroboscopically presented pairs of visual patterns are shifted in space and their contrast polarity is inverted simultaneously, motion is perceived in a direction reversed to that of the stimulus. They are driven by luminance changes. These tend to be strongest in the fovea and do not disappear when viewed through a pinhole aperture.

In Fig. 1, we show different variations of a rotation illusion in different colors, with the bottom row being the mirrored version of the top row. The illusory rotation is dependent on the colors and relative contrast of the colors, and motion is seen from lightest tint → black → darkest tint → white. The rotation is also dependent on the background color. Printed on paper with a reasonable quality and illuminated by a white source, one will perceive the same rotation as on a screen. The effective color contrast will, however, be a combined result of the printed paper's reflectance spectra and light spectrum. Colored light will affect the effective color contrasts, and depending on the light spectrum, may decrease it or reverse it slightly or dramatically. Please note that the assumption that illumination does not affect the contrast between the object and the background

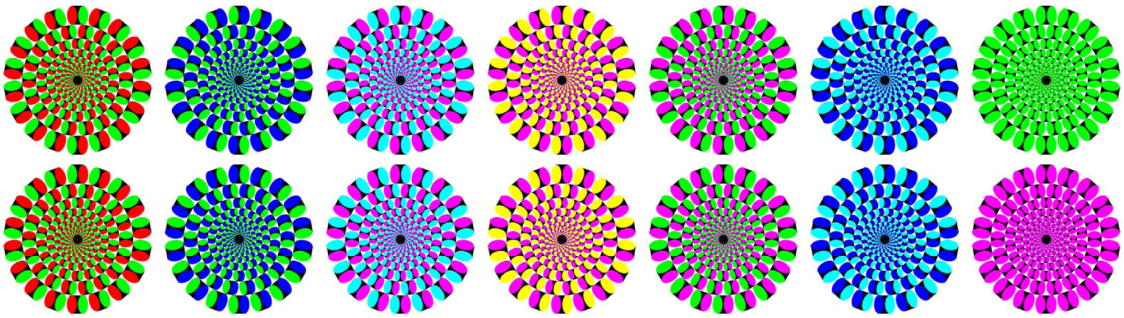

Fig. 1. Stimulus set, first row (RG, GB, CM, MY, GM, and BC) and control pattern GG. Second row with the reversed stimuli (GR, BG, MC, MY, MG, and CB) and control pattern MM. Since the color contrasts are reversed for the top and bottom stimuli, they seem to rotate in the opposite directions. We recommend the reader print out this figure (see Visualization 1 and the rendered simulation of the stimuli in Visualization 4) and try RGBCMY illumination changes using either an LED lamp or using a screen with uniformly colored slides in a dim room.

[15] is only true in full spectrum (say, white) homogeneous light fields. In spatially and directionally varying light fields and in colored light, contrast reversals can easily happen due to light–material/object interactions. The effective luminance of a single patch of colored material is the result of the spectrum of illumination and spectral reflectance of the print. The effective luminance can be as high as the spectral reflectance if the illumination contains all wavelengths of that reflectance profile or as low as zero if there is no overlap at all between those spectra. For example, red illuminated by red remains red, but when red is illuminated by blue it becomes black. Blue illuminated by blue remains blue, but when blue is illuminated by red it becomes black. So blue–red patterns will switch contrast if the illumination switches from blue to red and vice versa.

More subtle contrast and color variations will happen for cyan, magenta, and yellow, since those are mixing colors. For example, cyan illuminated by cyan remains cyan and when it is illuminated by magenta it becomes blue. Yellow illuminated by cyan becomes green and when yellow is illuminated by magenta it becomes red. So cyan–yellow patterns will switch contrast and color contrast from cyan–green to blue–red if the light switches from cyan to magenta. A white background will change to the illumination color, which can cause a brightness contrast and color contrast to become higher or lower.

LED sources have quite narrow spectra (compared to incandescent sources with filters) and therefore can induce quite strong color effects. Red–blue under red LED light, for instance, will show up as red–(almost) black, while a under blue LED light it will become (almost) black–blue. This will induce a rotation change. Since the induced changes are dependent on the colors of the print and of the LED source, it is possible to drive the rotation changes by tuning the colors.

In this paper, we test whether illumination-induced illusory rotations are robust across individuals and whether they agree with predictions made on the basis of effective color contrast. The main underlying mechanism concerns the reverse phi effect, and the novelty of this study lies in the induction of powerful dynamics by light–material (print) interactions in a real setting (not on a screen). The technical key element concerns brightness and color contrast changes or even reversals, which can be predicted well in a simple model.

2. METHODS

A. Participants

Twenty-one volunteer participants (18 female, age range 18–36, mean = 26.2, SD = 5.32) were recruited using the psychology department's recruiting system. Data were acquired within two weeks. All participants had normal or corrected-to-normal visual acuity and normal color vision. They gave written consent prior to the start of the experiment. The participants were paid for their participation or received research credit. Two participants were expert observers from our lab, but they were naive to the purpose of the experiment. The study was approved by the local ethics committee (LEK FB06) and was conducted in accordance with the ethical standards put forward in the Declaration of Helsinki. One participant reported to have not seen any rotation on any of the trials and was excluded from the analysis below.

B. Stimuli

Stimuli were generated in Mathematica using part of the code of the Spinning Circles Wolfram demonstrations project by Beeler and Farmer [16]. They consisted of concentric patterns of repeating colored elements. Each element had two elliptical chromatic regions that differed in color and a wedged-in black area. In total, there were seven such patterns and their reversals and two control patterns, for which the two chromatic regions were of identical color (Fig. 1). The size (diameter) of the stimulus was about 12 cm, which corresponds to an approximately 10 deg visual angle at a viewing distance of about 70 cm. The size of the individual elements ranged from 1.7 cm (largest) to 0.2 cm (smallest).

Patterns were printed from a pdf file on standard white printing paper using a Xerox AltaLink C8035, 5.9.0 printer, with settings for Acrobat Color Management, working sRGB, and Preserving CMYK primaries. As illumination for the patterns served a computer monitor (Dell UltraSharp 27 4 K, 1960 × 1080) with brightness and contrast set to 100 %, the color of the illumination could be varied by changing the color of a full-screen window using PsychoPy [17] routines. There were six illumination colors (defined in PsychoPy, in which colors are expressed as deviations from a gray screen, and −1 is the maximum decrement from gray, and +1 is the maximum

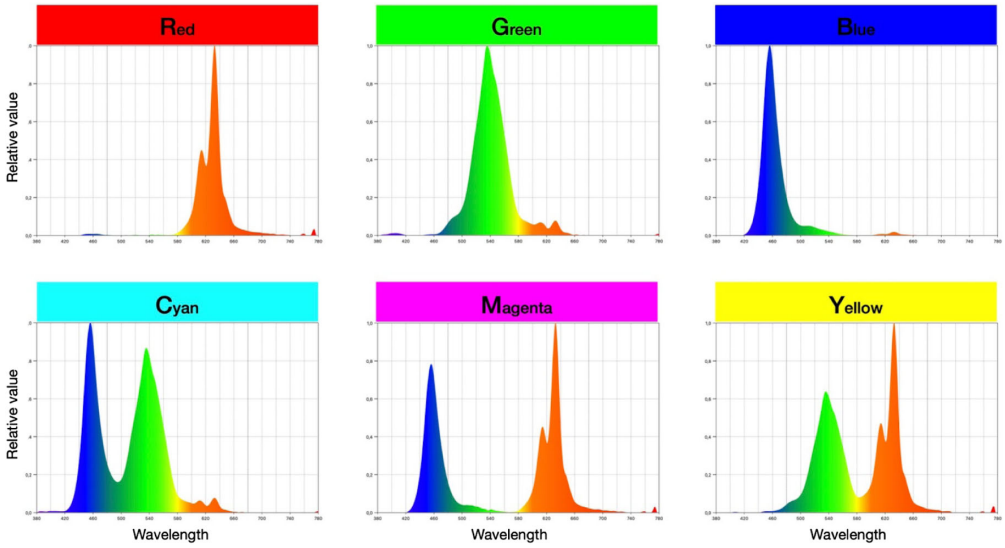

Fig. 2. Illumination spectra of the LCD monitor-generated lights used in the experiments.

increment above gray): red R (1, −1, −1), green G (−1, 1, −1), blue B (−1, −1, 1), cyan C (−1, 1, 1), magenta M (1, −1, 1), and yellow Y (1, 1, −1. There were five possible transitions between these illumination colors: R to G, G to B, B to C, C to M, and M to Y. We picked a subset of printed patterns to demonstrate the effect while not making the experiment too long. The illumination spectra for each light color are shown in Fig. 2, and illuminance levels, peak and dominant wavelengths, and purity are given in Table 1. It is clearly visible that the LED lighting was narrow-banded, which is typical for LED lighting and, in practice, allows easy spectral tuning in a coarse-grained "spectral" RGB/CMY framework. Each of the 14 patterns was shown under every illumination transition resulting in a total of 5 × 14 trials per participant.

C. Apparatus

The printed patterns were placed on a desk on a 20.5 cm tall pedestal at a distance of approximately 70 cm. The computer monitor was rotated into a vertical orientation and placed slightly to the left of the stimulus. Figure 3 shows two views of the experimental setup.

Table 1. Illuminance Levels, Peak and Dominant Wavelengths, and Purity of the LCD Monitor-Generated Lights

	Red	Green	Blue	Cyan	Magenta	Yellow
Illuminance [lux]	67.3	199	21.9	226	80.5	270
Peak wavelength [nm]	633	536	456	456	633	633
Dominant wavelength [nm]	618	546	465	494	551	570
Purity [%]	96.5	86.1	93.6	39.5	73.3	89.5

D. Procedure and Task

After providing written consent, participants were seated at the table, and the room lights were turned off except for a small lamp placed behind the screen in the background. Then, the experimenter placed a practice stimulus (Fig. 3, right panel) on the pedestal and read the instructions to the participant: "In this experiment, you will see colorful patterns like this. During the experiment, the color of the light falling on the printed pattern will change. When this happens please indicate whether the pattern rotated clockwise by pressing the right arrow key, or counterclockwise by pressing the left arrow key.

Fig. 3. Two views of the setup under normal (left) and experimental illumination conditions (middle), with green illumination coming from the screen toward the stimulus. The screen was placed such that it illuminated the stimulus homogeneously, and the observer (here, author S. P.) saw the back of the screen with the stimulus just behind and aside it. The experimenter was sitting behind the right backscreen and replaced the stimulus after running each set of RGBCMY lightings. The right panel shows the practice stimulus we designed. This pattern was not used in the actual experiment.

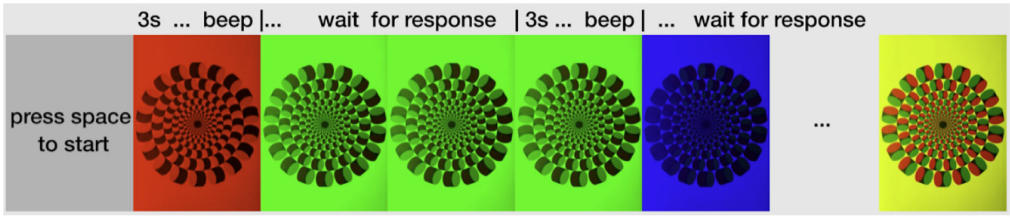

Fig. 4. Typical sequence of trials for one stimulus (RG). The participant started the experiment by pressing the space bar, and the red light illuminated the paper for 3 s. At the end of the 3 s, a sound occurred to signal that an illumination change was about to occur. After the beep, the illumination changed to green and remained so until the participant responded using the arrow keys on the keyboard. The press of a key was combined with a second sound to provide feedback to indicate that now the next trial had started. The green light stayed on for 3 s, followed by a sound to signal the transition to the next light color (blue) and, again, remained blue until the observer responded. This was repeated until all five illumination transitions (R → G, G → B, B → C, C → M, M → Y) were completed.

Press the down arrow if the pattern didn't move, press the up arrow if you like to repeat a given illumination change, which will start after pressing the spacebar. Whenever you press an arrow key, you will hear a beep, you will hear another type of beep just before each change in light color. You can practice now." Following this, participants were allowed to practice until they felt comfortable with the procedure. The experimenter replaced the practice stimuli with one of the experimental patterns, started the experimental program again, turned off the small background light, and asked the participant to proceed with the trials by pressing the spacebar. The order of patterns (Fig. 1) was randomized between the participants. The order of the illumination color transition was the same for every printed pattern. Figure 4 illustrates a sample trial in the experiment (see also see Visualization 2). In the supplementary material, we also provide the stimuli.tiff to print (Visualization 1) and a ScreenColors.pdf (Visualization 3) for illuminating the printed stimuli using a screen, which can be used to try this at home or to see the computer-rendered version (Visualization 4). Again, our model will hold for any pattern-light change combination. This can be a fun exercise for the interested reader to do (since it is really very simple to produce this illusion).

3. ANALYSIS

A. Data

For every pattern-illumination change condition, we collected the responses about the perceived rotation [counterclockwise ccw (1), clockwise cw (−1), none (0)], as well as the response time. For the "inverted patterns" (Fig. 1, second row), we inverted the rotation responses and treated them as two repetitions of the same condition. From the rotation responses, we computed a "cw" rotation index by counting across observers the number of cw and ccw responses, subtracting them from each other, and dividing the difference by the total number of responses. We compared the cw index (CWI) to a simple and a full model that each predicted perceived rotation on the basis of changes in luminance contrast (see below). We also assessed the observer consistency and response time for all light pattern combination conditions.

B. Models

The model uses a very coarse-grained spectral approach, assuming perfect separation between the red, green, and blue spectra and assuming that cyan, magenta, and yellow are simple superpositions of red, green, and blue, so $C = G + B$, $M = R + B$, and $Y = G + B$. This is indeed the case for the light, as can be seen in Fig. 2. For a first, coarse but simple model and for understanding the mechanisms, we also assume this to be the case for the materials. Then, the relative values of the "course-grained spectra" for both lighting and prints can be simplified by describing the energy in the three bins and can be modeled as R (0,0,1), G (0,1,0), B (1,0,0), C (1,1,0), M (1,0,1), and Y (0,0,1), which we will call spectral coordinates below. Effective spectral coordinates were then determined by a binary filtering operation of print and light spectral coordinates, resulting in the colored letters in Table 2, with K meaning black or (0,0,0). (See also Visualization 7, Visualization 8, Visualization 9, Visualization 10, Visualization 11 and Visualization 12 for computer-rendered versions of the stimuli under RGBCMY lighting.)

Assuming the luminance is weighted according to

$$L = 0.3R + 0.6G + 0.1B,$$

we calculated the effective contrast (the numbers in Table 2) as

$$\text{Contrast} = (L_1 - L_2) / (L_1 + L_2),$$

where L_1 is the left letter's spectral coordinates, and L_2 is the right letter's spectral coordinates.

If the light switches from one color to another, the effective contrast might change, with a change toward more negative values predicting an anti-clockwise rotation and towards more positive values a clockwise rotation. The larger the change, the more powerful the rotation is predicted to be. For instance, for the first stimulus RG, the first row of Table 2 predicts that if the light turns from red to green, the stimulus will go from red–black to black–green and the effective contrast from 1 to −1 (see also Fig. 4, the left part), predicting a powerful anti-clockwise rotation. Then with the light turning from green to blue, the effective contrast goes to zero, predicting a less powerful clockwise rotation, and so on. In order to compute the clockwise index for the model, we took the difference in effective contrast between two lights and divided it by 2, e.g., for the above R-to-G light change example, the cw index would be $(-1-1)/2 = -1$.

Table 2. Relative Luminance Contrasts for the Effective Colors Using a Coarse-Grained Spectral Approach[a]

	LIGHT COLORS & RESULTING PRINT PATTERN CONTRASTS												
PRINT	White	Red		Green		Blue		Cyan		Magenta		Yellow	
RG	-0.3	RK	1	KG	-1	KK	0	KG	-1	RK	1	RG	-0.3
RB	0.5	RK	1	KK	0	KB	-1	KB	-1	RB	0.5	RK	1
GB	0.7	KK	0	GK	1	KB	-1	GB	0.7	KB	-1	GK	1
CM	0.3	KR	-1	GK	1	BB	0	CB	0.8	BM	-0.6	GR	0.3
CY	-0.1	KR	-1	GG	0	BK	1	CG	0.1	BR	-0.5	GY	-0.2
MY	-0.4	RR	0	KG	-1	BK	1	BG	-0.7	MR	0.1	RY	-0.5
RC	-0.4	RK	1	KG	-1	KB	-1	KC	-1	RB	0.5	RG	-0.3
RM	-0.1	RR	0	KK	0	KB	-1	KB	-1	RM	-0.1	RR	0
RY	-0.5	RR	0	KG	-1	KK	0	KG	-1	RR	0	RY	-0.5
GC	-0.1	KK	0	GG	0	KB	-1	GC	-0.1	KB	-1	GG	0
GM	0.2	KR	-1	GK	1	KB	-1	GB	0.7	KM	-1	GR	0.3
GY	-0.2	KR	-1	GG	0	KK	0	GG	0	KR	-1	GY	-0.2
BC	-0.8	KK	0	KG	-1	BB	0	BC	-0.8	BB	0	KG	-1
BM	-0.6	KR	-1	KK	0	BB	0	BB	0	BM	-0.6	KR	-1
BY	-0.8	KR	-1	KG	-1	BK	1	BG	-0.7	BR	-0.5	KY	-1

[a]Vertically, the basic color combinations of the print. Horizontally, the basic light colors. In the table, the letters and their colors depict the effective color combinations of the print × lighting, using a coarse spectral three-band RGB approach. To the right of those depicts the signed color contrast.

Figure 5A shows model predictions of the simple model for all conditions, with red colors denoting clockwise and blue colors denoting counterclockwise rotations.

The above coarse-grained spectral approach was used for its simplicity and explanatory power of human ecology [10,18–20]. Once the fundamental mechanisms are understood, it is relatively easy to extrapolate the methods to accurately measure the finer resolution spectral data. Since we expected the print spectra to show broader and less peaked spectra, we also checked predictions in two other ways. Please note that because most object colors have rather smooth spectra, they can be described by the energy in the three bins (BGR) for explaining the light-print interactions in a human ecology. We printed out a color swatch with a large 9 cm × 9 cm square of the used colors, using the same printing procedure and settings as for the stimuli. First, we measured the "spectral coordinates" using an albedo app, the "sister app" of the HydroColor app [21], using a photographic 18% gray card for calibration and a stable white full spectrum light source. This gave the following coordinates (ordered as BGR, like the above): R (0.2, 0.0, 0.0), G (0.0, 0.2, 0.1), B (0.0, 0.1, 0.2), C (0.0, 0.2, 0.3), M (0.3, 0.0, 0.1), and Y (0.8, 0.7, 0.0). Then, we repeated the modeling calculations above with

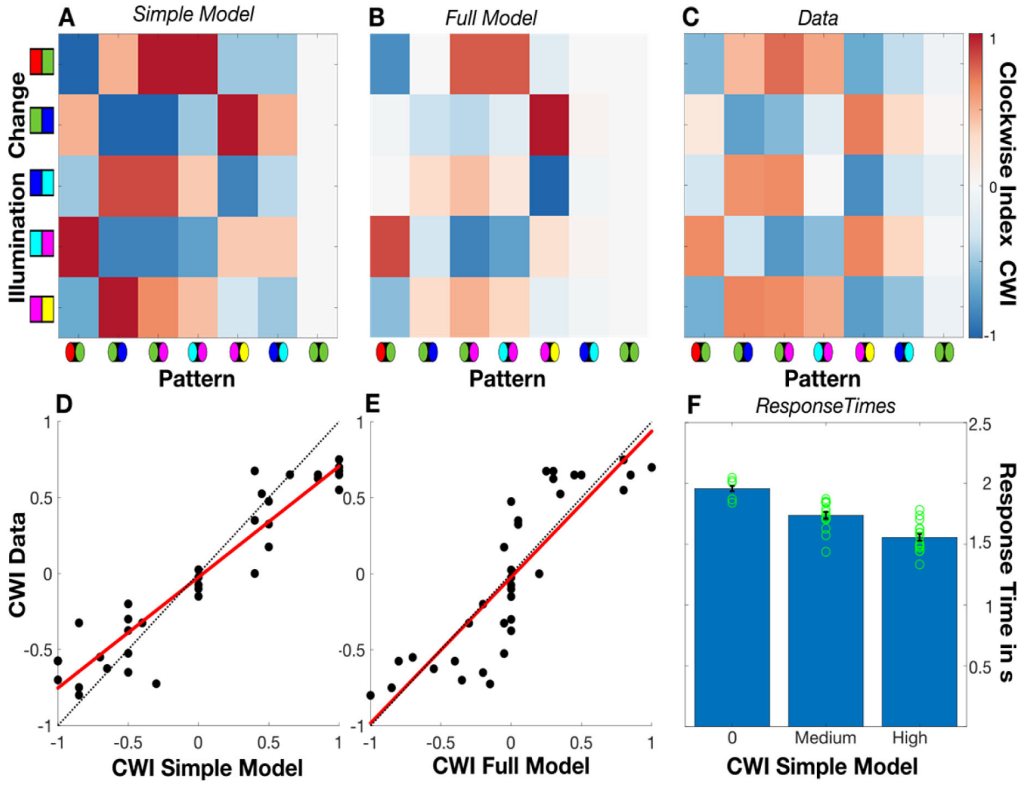

Fig. 5. Clockwise index (CWI) shown for model predictions and participant data. A value of 1 means this that stimulus was always seen as rotating clockwise. Conversely, a value of −1 means that this stimulus was always seen as rotating counterclockwise. A value of 0 means that this stimulus was not seen as rotating. The x-axis denotes the color of the printed patterns, and the y-axis denotes the illumination transition under which the pattern was observed. (A) CWI predictions of the simple model, (B) CWI predictions of the full model, (C) CWI obtained from the observer data, and (D) observers' CWI predicted by the simple model. The red line is the regression line, and the black dotted line is the identity line. (E) Observers' CWI predicted by the full model. (F) Response times binned by the clockwise index magnitude. Error bars are 1 standard error of the mean. Green dots are individual response times (averaged for forward-reverse pairs and the two control conditions GG and MM).

these coordinates. Figure 5B shows the predictions of the full model.

4. RESULTS

Overall, participants reported to perceive the patterns under light changes as rotating. Only one participant did not perceive any rotation at all. To formally test for a rotation effect, we conducted a t-test, testing against the null hypothesis that the absolute value of the CWI was equal to 0 (not including the two control conditions GG and MM), $t(29) = 14.51$, and $p < 0.0001$ (the mean of the absolute value of the CWI was 0.53). In contrast, the mean value of the CWI in the control conditions was −0.07, and the t-test against the zero mean was not significant, $t(4) = -2.15$ and $p = 0.0978$. Figure 5C plots the CWI for each condition. These data were well predicted by both simple and full contrast models, with an adjusted R^2 0.889 and $p < 0.0001$ and $R^2 = 0.722$ and $p < 0.0001$, respectively. Figures 5D and 5E plot the CWI obtained from the data as a function of simple and full model predictions, respectively.

Each observer essentially repeated the same condition twice (forward and reversed), so we can assess qualitatively intra-observer consistency by first flipping the responses to the reversed patterns and then comparing the result with the forward patterns. Ideally, the responses should be the same. However, Fig. 6A shows that participants were not always consistent for forward and reverse judgments. In particular, observers 2, 7, 10, 12, and 20 seemed to have responded inconsistently when seeing the same pattern. As a result, the average response of these participants for nearly all conditions (five light transitions × seven patterns) amounts to zero (Fig. 6B). These observers also correlate lower with other participants (Fig. 6C).

The overall consistency of judgments for a given condition is shown in Fig. 6D. The consistency was computed by first counting the number of cw, ccw, and "no rotation" responses for each condition. Then, the maximum of counts was determined, and finally, this maximum was divided by the total responses (two for each participant). The color-coded results are shown in Fig. 6D. The model CWI magnitude predicted observer consistency, with an adjusted $R^2 = 0.207$ ($p < 0.006$) and $R^2 = 0.422$ ($p < 0.0001$) for the simple and full model, respectively. Note that this regression analysis did not include the control conditions, for obvious reasons.

Finally, we checked whether the predicted strength of the rotation effect would cause differences in response times. The argument being that the absence of or a stronger effect might be "easier" and hence faster to judge than a small effect. To do this, we split the stimulus conditions into three bins according to the predicted CWI magnitude (simple model). Sixteen

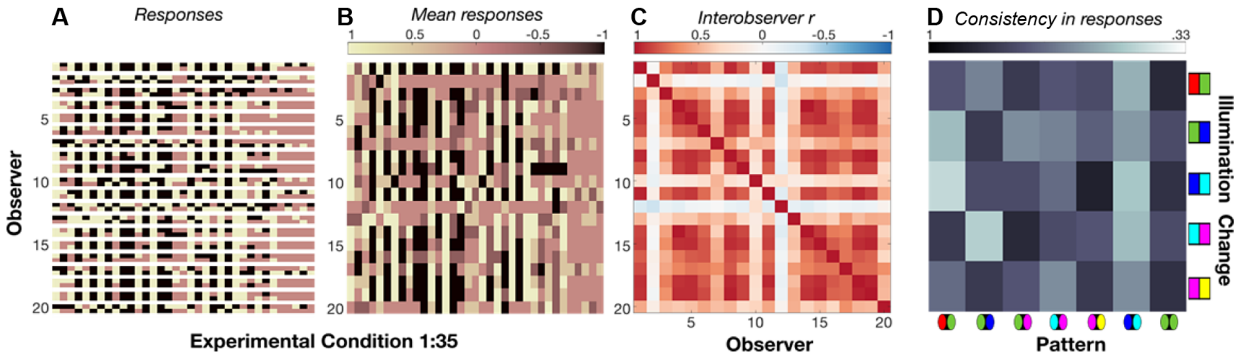

Fig. 6. Intra- and Interobserver consistency. (A) Observer responses (−1, clockwise; 1 counterclockwise; 0, no rotation) are depicted for all 35 (seven patterns × five illumination transitions). The last five columns are the control patterns (GG and MM) where no rotation should have been perceived. Each observer saw a printed pattern under a given illumination change twice, in its forward and reverse versions (see Fig. 1). Responses for the reverse condition were inverted (second row for each observer). Consistent observers would have the same color across the two rows. Individual observers are separated by a white line in this plot. Colors are as in panel B. (B) Observer responses averaged over the two occurrences of a condition. Observers that respond maximally inconsistent in a given condition average to zero. (C) Inter-observer correlations. Intra-inconsistent observers, e.g., observers 2 and 12, also correlate low with the majority of observers. (D) Observer consistency for each condition. The lower bound on consistency was 0.33 (white), implying that only one-third of the observers responded in the same way. Black implies that all observers gave the same response.

conditions had high predicted CWI magnitudes between 1 and 0.6 (absolute value), 14 conditions had a predicted medium CWI (between 0.2 and 0.6), and five conditions had a predicted CWI of 0. Comparing response time across bins using a one-way ANOVA with unequal sample sizes, we found significant differences, $F(2, 32) = 24.1$ and $p < 0.0001$ (Fig. 5F). Post hoc comparisons revealed significant differences $p < 0.003$ between all three bins (means: 1.95, 1.73, and 1.55 s for 0, medium, and high magnitude CWIs, respectively). Using the CWI magnitude computed by the full model to bin response times, we obtained similar results [$F(2, 32) = 12.41$, $p = 0.0001$, means: 1.88, 1.66, and 1.54 s for 0, medium, and high magnitude CWIs, respectively. The difference between medium and high magnitude CWI response times did not reach significance $p = 0.127$).

5. CONCLUSION AND DISCUSSION

Printed illusory rotation illusions with color contrast under changing colored LED illumination drive illusory clockwise and anti-clockwise rotations. Our experiment confirmed these powerful percepts and, moreover, also confirmed our model predictions based on the changes in effective luminance contrast. In the experiment, observers indicated whether they perceived clockwise, counterclockwise, or no rotations while freely viewing printed colored patterns illuminated by a chromaticity-changing LED computer screen. The overall rotation effect was summarized by a CWI that essentially provides a measure of how many participants saw a clockwise (or counterclockwise) rotation for a given stimulus. While we did find interobserver differences, our model predicted CWI data across participants and conditions rather well.

Our models predicted CWI in the ranges of −1 (ccw rotation) to 1 (cw rotation), where the strength of the predicted rotation effect (CWI) scales with the magnitude of the luminance contrast change. We did not measure the perceived strength of the rotation effect directly, since the task was a three-way alternative forced choice. However, we reasoned that "effect strength" might be derived indirectly from the CWI data. A CWI of 1 implies that all participants perceived a clockwise rotation, and a CWI of −1 means that all participants perceived a leftward rotation. If that were the case, we could argue that the visual rotation effect is very strong. Conversely, a value of 0 means that the rotation effect is "difficult to perceive" or "weak in amplitude," as for example, the predicted CWI of the CM pattern under the BC illumination transition in Fig. 5B. In that case, we might expect mixed responses, observer consistency would be low, and the corresponding CWI might be 0. However, we also included catch trials of same-color patterns in the experiment, and also here the CWI would be predicted to be 0, yet here we would expect all participants to clearly *not* see a rotation, i.e., they would be highly consistent in their judgment. The consistency measurements in Fig. 6D qualitatively show the expected pattern, e.g., low consistency in responses for the CM pattern–BC illumination combination, high consistency responses for the control condition (last column in Fig. 6D), and high consistency responses for "easy" conditions, e.g., the RG pattern under the RG illumination transition. Quantitative regression analysis confirmed a significant relationship between the predicted CWI magnitude and the observers' consistency.

Yet the range of CWI data in Fig. 5C suggests that in no single condition did all observers give perfectly consistent answers. This was at first surprising to us, since all but one participant reported to perceive rotations. To understand this better, we inspected how consistent participants were within themselves and across each other. A handful of observers responded in a surprising pattern, notably, they responded in opposite ways when encountering the same pattern (Figs. 6A and 6B). This would not be unexpected for "hard-to-perceive" conditions [e.g., the one mentioned above, column 9 in Figs. 6A and 6B, and the column 18 CM (pattern)–BC (illumination) condition] but should not occur in conditions where a strong CWI effect is predicted, e.g., the first column in Figs. 6A and 6B [the RG (pattern)–RG (illumination) condition]. Moreover, the same individuals often also indicated that they perceived rotations in the control conditions, much more frequently than "consistent"

participants. What might be the reason for these inconsistent response patterns? One possibility is that they did not do the task sincerely or that they "expected" a rotation on every trial and responded accordingly. Since participants had the possibility to repeat illumination transitions, we can rule out that they did not see the illumination change, for example, because they blinked at the moment of illumination transition. Unsurprisingly, inconsistent participants also tended to correlate lower with other participants (including other inconsistent participants, e.g., participants 2, 12, or 20). In future experiments, one could obtain not only forced choice direction judgments but also the measurements of the perceived magnitude of the rotation. This would allow a better assessment of individual perceptual variations and the prediction of individual CWIs by the contrast model(s).

Also, one observer did not see the rotation. We asked this observer to come back to the lab and showed the rotating snake illusion, four-stroke reverse phi and two-stroke reverse phi. This observer reported seeing motion for the rotating snakes, four-stroke reverse phi-motion, and phi-motion, all in the expected direction. We showed (repeatedly) the RG and GR stimuli for the red–green light changes. However, the observer reported not being able to perceive any rotation. We moved the stimulus to a greater viewing distance, yet this did not change the perception. We are puzzled by these observations.

The coarse-grained spectral approach using just three bins predicted the pattern and strength of the responses well. The simple model with ideal spectral reflectance coordinates correlated well with the CWI data, showing a linear trend. The full model also correlated quite well with the CWI data but with a lower R^2 and the scatter plot showing a sigmoid pattern instead. The full model was generated on the basis of coarse-grained spectral measurements, which showed, as predicted, that the albedo of the printed colors was actually lower than the colors of those stimuli on screen. The full model consequentially showed many lower-effective contrast values and therefore lower CWI predictions. The scatter plot in Fig. 5E shows how many of the model predictions cluster around zero. However, the data for those predictions show a steep change in the CWI data, indicating that although the effective luminance contrast changes were small in the range, the illusory rotations, overall, still triggered stronger responses. This suggests that the actual color effects boost the illusory rotations, as shown in [8] for blue–yellow versus red–green (although for a different mechanism, namely, peripheral drift, while in the current study, the main mechanism is foveal) and that the basic variations of our testing paradigm might form a manner to further our understanding of these mechanisms. In addition, the background color affects the induced rotation strength, which needs further investigation. The paper stimulus background was white and in the experiment changed according to the illumination color. Darker backgrounds, however, attenuate the effect (see Visualization 5 and Visualization 6 for computer-generated versions of the stimuli with gray and black backgrounds under RGBCMY lighting).

The tested effects concern the perceived rotation directly after the illumination changed color. Several observers noted that rotations persisted after that, though less strong/fast/powerful. Disentangling the direct and persisting temporal effects, how they are related to contrast and luminance and neural mechanisms, can be related to the works of Conway *et al*. [6] and Backus and Oruç [4] but would need further research and complementary experiments using, e.g., nulling methods. The illumination modulations presented here can be used to further investigate how color can enhance or attenuate the illusions. In future research, we will test different temporal variations, e.g., ramps of illumination color changes, and different spectral variations, e.g., metameric illumination and print combinations, also for other colored rotation illusions. We would like to invite the reader to try.

Since these new illusory rotations are highly predictable, they allow for applications in which combinations of printed imagery and illumination can be used, adding a perceptual dynamic layer without having to use expensive screens or actual kinetics. For instance, printing these patterns on road signage and illuminating them with colored light will drive rotation perception once hit by white car headlights. The current demonstrations are, however, quite intense to look at, so our future research will test how we can induce the effects with less dramatic spectral changes. First explorations with CCT-varying lamps were promising, and future research will include testing effects under metameric white illuminations.

Funding. Deutsche Forschungsgemeinschaft (222641018–SFB/TRR 135); Hessisches Ministerium für Wissenschaft und Kunst.

Acknowledgment. Funding was provided by the Deutsche Forschungsgemeinschaft (DFG, German Research Foundation), project number 222641018–SFB/TRR 135, Project B8 (KD), and by the Hessisches Ministerium für Wissenschaft und Kunst (HMWK; project "The Adaptive Mind") (KD).

Disclosures. The authors declare no conflicts of interest.

Data availability. Data underlying the results presented in this paper are not publicly available at this time but may be obtained from the authors upon reasonable request.

REFERENCES

1. A. Kitaoka, "The Fraser-Wilcox illusion and its extension," in *The Oxford Compendium of Visual Illusions*, 1st ed., A. G. Shapiro and D. Todorovic, eds. (Oxford University, 2017), pp. 500–511.
2. A. Kitaoka, "Color-dependent motion illusions in stationary images and their phenomenal dimorphism," Perception **43**, 914–925 (2014).
3. A. Kitaoka and H. Ashida, "Phenomenal characteristics of the peripheral drift illusion," Vision **15**, 261–262 (2003).
4. B. T. Backus and İ. Oruç, "Illusory motion from change over time in the response to contrast and luminance," J. Vis. **5**(11):10, 10 (2005).
5. L. Atala-Gérard and M. Bach, "Rotating snakes illusion—quantitative analysis reveals a region in luminance space with opposite illusory rotation," i-Perception **8**, 2041669517691779 (2017).
6. B. R. Conway, A. Kitaoka, A. Yazdanbakhsh, *et al.*, "Neural basis for a powerful static motion illusion," J. Neurosci. **25**, 5651–5656 (2005).
7. M. Bach and L. Atala-Gérard, "The rotating snakes illusion is a straightforward consequence of nonlinearity in arrays of standard motion detectors," i-Perception **11**, 2041669520958025 (2020).
8. M. Uesaki, A. Biswas, H. Ashida, *et al.*, "Blue-yellow combination enhances perceived motion in Rotating Snakes illusion," i-Perception **15**, 20416695241242346 (2024).
9. C. R. L. Cantor, H. J. Tahir, and C. M. Schor, "Is the Rotating Snakes an optical illusion?" J. Vis. **10**(7):824, 824 (2010).
10. M. Bach, "Reverse phi illusion," Michael Bach, 2024, https://michaelbach.de/ot/mot-reversePhi/.

11. O. J. Flynn and A. G. Shapiro, "The perpetual diamond: contrast reversals along thin edges create the appearance of motion in objects," i-Perception **9**, 2041669518815708 (2018).
12. A. Kitaoka, "Configurational coincidence among six phenomena: a comment on van Lier and Csathó (2006)," Perception **35**, 799–806 (2006).
13. S. M. Anstis, "Phi movement as a subtraction process," Vis. Res. **10**, 1411 (1970).
14. R. L. Gregory and P. F. Heard, "Visual dissociations of movement, position, and stereo depth: some phenomenal phenomena," Q. J. Exp. Psychol. Sect. A **35**, 217–237 (1983).
15. R. O. Brown, "Backgrounds and illuminants: the yin and yang of colour constancy," in *Colour Perception: Mind and the Physical World*, R. Mausfeld and D. Heyer, eds. (Oxford University, 2003).
16. V. Beeler and J. Farmer, "Spinning circles optical illusion," Wolfram demonstrations project, 2025," https://demonstrations.wolfram.com/SpinningCirclesOpticalIllusion/.
17. J. W. Peirce, "PsychoPy—Psychophysics software in Python," J. Neurosci. Methods **162**, 8–13 (2007).
18. J. Koenderink, A. van Doorn, and K. Gegenfurtner, "Colors and things," i-Perception **11**, 2041669520958431 (2020).
19. J. Koenderink, A. van Doorn, and K. Gegenfurtner, "RGB colors and ecological optics," Front. Comput. Sci. **3**, 630370 (2021).
20. C. Yu, M. Wijntjes, E. Eisemann, *et al.*, "Effects of inter-reflections on the correlated colour temperature and colour rendition of the light field," Light. Res. Technol. **55**, 772–793 (2023).
21. T. Leeuw and E. Boss, "The HydroColor app: above water measurements of remote sensing reflectance and turbidity using a smartphone camera," Sensors **18**, 256 (2018).